Synthesis and structural characterization of $CuAl_2O_4$ spinel with an unusual cation distribution

Yajie Liu,[1,2] Shaojun Qing,[2] Xiaoning Hou,[2] Gang Feng,[3] Rongbin Zhang,[3] Xiang Wang,[3] Shanmin Wang,[4] Zhixian Gao[2*] and Hongwei Xiang[2]

1. College of Chemistry and Chemical Engineering, Jinzhong University, Jinzhong 030619, China

2. Institute of Coal Chemistry, Chinese Academy of Sciences, Taiyuan 030001, China

3. Institute of Applied Chemistry, College of Chemistry, Nanchang University, Nanchang 330031, China

4. Department of Physics, Southern University of Science and Technology of China, Shenzhen 518055, China

E-mail: gaozx@sxicc.ac.cn

Abstract: A $CuAl_2O_4$ spinel with unusual cation distribution has been synthesized for the first time by the solid phase reaction of copper hydroxide and pseudo-boehmite with both stoichiometric (Cu/Al = 1/2) and non-stoichiometric (Cu/Al = 1/3) ratios. Instead of characterizing one cation for the determination of cations distribution as generally performed in previous literatures, both cations in the synthesized spinel have been characterized with ^{27}Al NMR for Al ions and EXAFS for Cu ions, respectively. The characterization data reveal that nearly all Al^{3+} ions are octahedrally coordinated while most Cu^{2+} occupy the tetrahedral sites, giving a $(Cu_{0.8})[Cu_{0.2}Al_2]O_4$ spinel which has been supported by the Rietveld refinement. The unusual cation distribution, which has been rarely reported before, presents abnormal site occupancies in Cu-Al spinel oxide. Hence, the findings of this work may invoke further explorations on other spinel oxides for targeting novel distinctive properties and applications.

Keywords: Spinel; Crystal structure; Nuclear magnetic resonance; Extended X-ray absorption fine structure.

1. Introduction

AB_2O_4 spinels have been found with wide applications in many areas such as catalysis [1,2], ceramics [3,4], magnetics [5,6] and batteries [7]. Spinel owns a face-centered cubic crystal structure with tetrahedral and octahedral interstices occupied by A^{2+} and B^{3+} cations [8].The unit cell of a spinel contains 32 oxygens and 24 cations, and it is universally assumed that 8 cations occupy 1/8 of the tetrahedral interstices while 16 cations occupy 1/2 of the octahedral interstices. Hence, the change of cation distribution will give a variety of spinels, and the structural formula is always written as $(A_{1-x}B_x)[A_xB_{2-x}]O_4$, where parenthesis and square bracket denote tetrahedral and octahedral sites, and A and B represent divalent and trivalent cations, respectively, and x is the degree of inversion, defined as the fraction of the tetrahedral sites occupied by trivalent cations. The two extreme forms are normal $(A)[B_2]O_4$ and inverse $(B)[AB]O_4$ spinel.

Using the structural formula, the cation distribution was obtained by XRD refinement or by characterization of the Cu^{2+} distribution as shown in the open literature. K.-I. Shimizu et al. [9] prepared stoichiometric Cu-Al spinel (containing 35 wt% Cu) by coprecipitation of copper acetate and aluminum nitrate with 10% NH_4OH at PH = 7-8, followed by calcining the precipitated precursor in air for 12 h at 1073 K. Using deconvolution analysis of Cu L_3-edge XANES, the ratio of Cu_{Td}/Cu_{Oh} (Tetrahedral/Octahedral) was determined to be 60/40. Another synthetic $CuAl_2O_4$ spinel containing 32.7 wt% Cu, prepared from a mixture of solutions of copper nitrate and aluminum sulfate, and fired at 450 ℃ for 6 h in a static air firstly, then fired under a dynamic oxygen gas flow at 952 ± 5 ℃ for 48 h, showed that 40% or 45% of the cupric ions were in octahedral sites, which was obtained by X-ray diffraction powder patterns (XRD) and X-ray absorption fine structure (EXAFS), respectively [10]. R. M. Friedigan et al. [11] have prepared $CuAl_2O_4$ by minimum solution impregnation of preformed γ-alumina supports by aqueous copper nitrate solutions. The preparations were calcined at 962 ℃ in static air. EXAFS fitting analysis showed that about 40% Cu^{2+} sited at the octahedral sites. R. A. Fregola et al. [12] prepared $CuAl_2O_4$ with analytical grade oxides by a flux growth method using $Na_2B_4O_7$ as flux media. The refinement of single-crystal XRD data illustrated that about 71% Cu^{2+} occupied the tetrahedral sites. It has also

been demonstrated that the cation distribution of $CuAl_2O_4$ showed a relatively small temperature dependence as compared to other spinels [13,14]. On the basis of these data, it can be found that $CuAl_2O_4$ is a largely normal spinel with an inversion degree of about 0.30-0.45 depending on the synthetic and post-treatment conditions.

Besides the above quantitative investigation methods, the disordering of $CuAl_2O_4$ was also illustrated by Al^{3+} coordination using ^{27}Al MAS NMR spectroscopy [15,16]. As shown by T. Mimani, both tetrahedrally and octahedrally coordinated aluminum ions were identified for a nanocrystalline $CuAl_2O_4$ spinel which was prepared by combustion method [15]. Similar result was later reported by E. Ghanti and R. Nagarajan for a $CuAl_2O_4$ prepared by hydrolysis of $CuAl_2(acac)_4(OiPr)_4$ [16]. However, these authors did the research qualitatively, and did not give a precise cation distribution.

Previously, we have synthesized a series of Cu-Al spinels by a simple and green solid phase reaction method. The sample with an atomic Cu/Al ratio of 1/2.5 calcined at 900 ℃ showed the best catalytic performance in methanol steam reforming for production of hydrogen [17]. During further investigations on the influence of calcination temperature, we find that an unusual $CuAl_2O_4$ spinel with all Al^{3+} sited at the octahedral site was synthesized at a high temperature of 1200 ℃. Moreover, comprehensive characterizations for both Cu and Al ions, rather than any one as performed with previous studies [10,11,18], are used in determining cation distribution in $CuAl_2O_4$ spinel.

We report an unusual $CuAl_2O_4$ spinel with abnormal site occupancies, and provide a new understanding in spinel structural characterization, which may be useful for exploring other special spinel with distinctive properties.

2. Experimental

2.1 Preparation process

Cu-Al spinel samples with a molar ratio of Cu/Al=1/2 or 1/3 were prepared by ballmilling of well-mixed copper hydroxide and pseudo-boehmite powders for 6 h, followed by calcining in static air muffle furnace from room temperature to a desired temperature at a rate of 3 ℃ min^{-1}, then cooled down naturally. The sample obtained at 1200 ℃ was denoted as CA_x, where x was Al/Cu ratio of the precursor. For comparison, a sample synthesized at 950 ℃ was named as CA_3-U.

2.2 Characterization

A comprehensive characterization was carried out with several techniques. Powder X-ray diffraction (XRD) patterns were collected on a Rigaku MiniFlex II desktop X-ray diffractometer operated at 40 kV and 40 mA with Cu-$K\alpha$ radiation source. The measurements were made in the 2θ angle range of 10º~80º with a 2θ step size of 0.01° and counting time of 2 s for each point.

H_2 Temperature-Programmed Reduction (H_2-TPR) was carried out with 30.0 mg sample on an automatic temperature-programmed chemisorption analyzer equipped with a thermal conductivity detector. The measurements was performed in 10% H_2/Ar flow (15 ml min^{-1}) with increasing temperature from 20 ℃ to 900 ℃ at a rate of 10 ℃/min. Under such conditions, the reduction of non-spinel Cu^{2+} can be separated from that of spinel, which enabled the calculation of the content of non-spinel Cu^{2+} species by area integration analysis.

The crystal dimension of CA_3 was investigated using a field emission Transmission Electron Microscope (HRTEM, JEM-2100F) operated at 200 kV.

The solid state nuclear magnetic resonance (NMR) was performed with a Bruker Avance 600 spectrometer in a nominal field of 14.2 T. The ^{27}Al spectra were observed using a magic angle spinning (MAS) probe with a 4.0 mm ZrO_2 rotor. A rotation frequency of approximately 13 kHz for CA_3 and CA_2, while 14 kHz for CA_3-U for the better resolution of tetrahedral Al^{3+} with spinning side band. The pulse excitation length and pulse interval were 0.4 μs and 1 s, respectively. Chemical shift values were referenced to $Al(NO_3)_3$ solution at 0 ppm.

Diffuse reflectance spectra were measured with a Cary 5000 spectrophotometer equipped with an integration sphere, and were recorded between 600-2000 nm at a scanning rate of 300 nm min^{-1} using dehydrated $BaSO_4$ as the dilute reagent.

The Cu K-edge XAFS spectra were measured in the transmission mode at the 1W1B endstation of the Beijing Synchrotron Radiation Facility (BSRF). The storage ring was operated at 2.5 GeV with current from 150 mA to 250 mA. A double crystal Si (111) monochromator was used for the experiments. The powder samples were pressed to reach the optimum absorption thickness ($\Delta\mu d \approx 1$, $\Delta\mu$ is the absorption edge jump and d is the physical thickness of the sample). X-ray absorption fine structure (XAFS) data were analyzed with the Demeter software package (ATHENA and ARTEMIS). Absorption curves were normalized and the XANES signals $\chi(k)$ were obtained after the removal of the pre-edge and post-edge background. The amplitude and phase shift functions

were obtained as $k^2\chi(k)$ with a Hanning window and curve fitting analysis was performed in R-space for first coordination shell with a hypothetical normal (Cu)[Al_2]O_4 spinel as the structural model. There were three free parameters for fitting: *N*, the coordination number; *R*, the distance and σ^2 the Debye–Waller factor.

XRD Rietveld refinement calculations were carried out for the determination of quantitative phase analysis and precise microstructural parameters of crystalline compounds. Cu-Al spinel and α-Al_2O_3 were well known as the face-centered cubic (Fd-3m(227)) and hexagonal crystal (R-3c(167)), respectively. The peak shape profiles were described by a pseudo-Voigt function, and the backgound was refined with a polynomial function. XRD data in the 2theta range of 10-80° was used for the refinement.

3. Results and discussion

Ball-milled Cu-Al mixtures with a Cu/Al = 1/2 or 1/3, which were used for the synthesis of stoichiometric and Al-rich spinels, respectively, were calcined in a wide temperature range of 800-1200 ℃. The formation of spinel is not observed below 800 ℃. With increasing calcination temperature, incorporation of Cu into the spinel structure increases, forming Al-rich spinel solid solutions. For example, samples synthesized at 950 ℃ are typical solid solution. However, at 1200 ℃ (CA_2 and CA_3), the formed solid solution transforms into stoichiometric $CuAl_2O_4$ spinel for both Cu/Al ratios. Therefore, both spinel samples and a typical solid solution sample calcined at 950℃ with a Cu/Al = 1/3 (CA_3-U) are shown in this work.

XRD patterns of samples all synthesized samples are shown in Fig. 1a. Single $CuAl_2O_4$ phase is observed with CA_2, while CA_3 contains both $CuAl_2O_4$ and α-Al_2O_3 crystal phases. For CA_3-U, only spinel phase is observed but with larger 2theta values (Fig. 1b), indicating the formation of Al-rich solid solution.

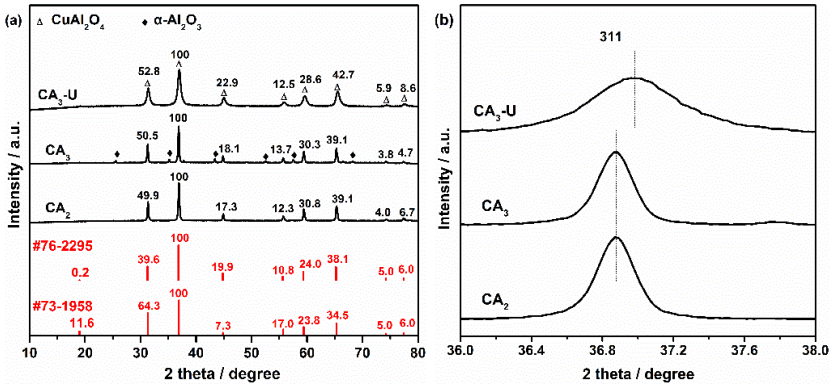

Fig. 1 XRD patterns of synthesized samples and reference samples (a), and details of the range 2θ = 36.0-38.0 (b).

$CuAl_2O_4$ phase shows very sharp and narrow reflections, and the six main diffraction peaks corresponding to different crystal planes at 2θ of 31.3° (220), 37.0° (311), 44.9° (400), 55.7° (422), 59.4° (511), 65.3° (440). However, the relatively wide peaks are observed in CA_3-U which was synthesized at a lower temperature (950 ℃).

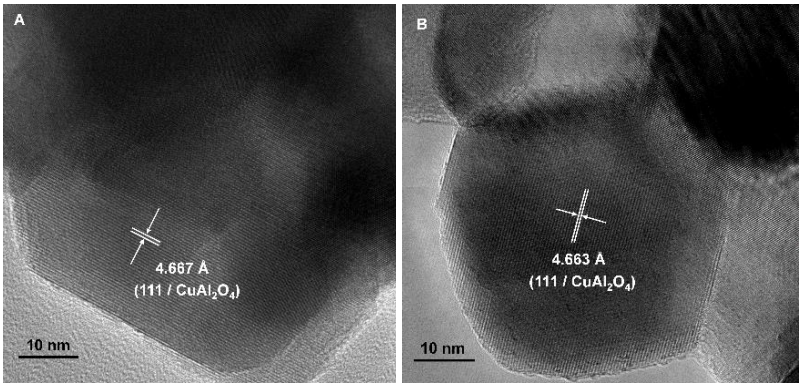

Fig. 2 HRTEM image of CA_2 (A) and CA_3 (B) (showing interplanar spacing of 111 plane of $CuAl_2O_4$).

With the samples CA_2 and CA_3, the cell constant of these spinels was determined, by Scherrer equation, to be 8.080 Å and 8.076 Å, respectively, which was further confirmed by HRTEM. As shown in Fig. 2, the interplanar spacing of 111 plane of $CuAl_2O_4$ are about 4.667 Å and 4.663 Å, giving a cell constant of 8.083 Å and 8.077 Å. A lower cell constant of 8.053 Å is acquried for CA_3-U. It worth noting that the cell constants of both CA_2 and CA_3 are very close to reference data of $CuAl_2O_4$ (#73-1958, 8.075 Å), indicating the formation of $CuAl_2O_4$ rather than solid solution. The crystal size of these spinels are about 34.9 nm and 34.5 nm, respectively.

As shown in Fig.1a, the relative peak intensities of both CA_2 and CA_3 are similar, but much different with the reference samples (PDF #76-2295, #73-1958). For example, the relative intensity of 220 plane with both CA_2 and CA_3 is about 50 %, while the literature data are 39.6%, 64.3% for #76-2295 and #73-1958, respectively, and the 52.8% for CA_3-U. As was pointed out by H. Furuhashi et al, the variation is correlated with cation distribution in spinels [19]. Thus, it can be concluded that both CA_2 and CA_3 may have a cation distribution different from literature results and CA_3-U.

The oxidation state of Cu ions was identified by H_2 temperature-programmed reduction (H_2-TPR), as shown in Fig. 3. The CA_3 exhibits a very small reduction peak centered at about 245 ℃ which is ascribed to non-spinel Cu species [17]. The area integration analysis shows about 99.6 mol% CuO exists as spinel phase for CA_2, and 99.8 mol% for CA_3. This implies that almost all Cu ions incorporate into spinel structure in CA_2 and CA_3.

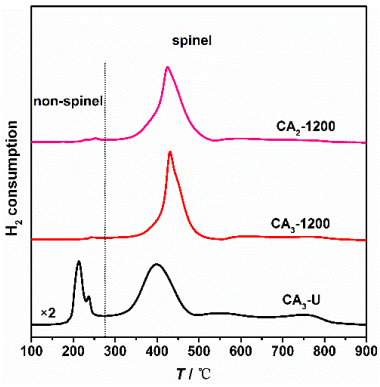

Fig. 3 H_2-TPR profiles of the CA_2 and CA_3, and CA_3-U

In addition, XRD Rietveld structural refinement results show that about 33.2% Al phase out of solid solution in CA_3. Therefore, the Cu/Al ratio in spinel phase of CA_3 is close to be stoichiometric, leading to a $CuAl_2O_4$ as the same with CA_2. However, about 18.7 mo% CuO phase exists in CA_3-U even though XRD do not show any CuO phase, implying the formation of Al-rich solid solution as illustrated by cell constant data.

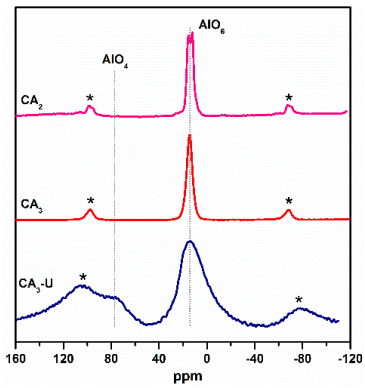

Fig. 4 ^{27}Al MAS NMR spectra of the CA_2 and CA_3, and CA_3-U (* indicates the spinning side bands).

Subsequently, Al^{3+} coordination in the synthesized samples is examined by ^{27}Al MAS NMR, and the results are shown in Fig. 4 and Table 1. A sharp and intense resonance signal at around d=14.0 ppm, attributed to six coordinated aluminum ions, is observed for all samples. However, signal attributed to tetrahedrally coordinated aluminum ions, which should appear at about 60-75 ppm [15,16,20-22], is not detected in both CA_2 and CA_3. For α-Al_2O_3 which is contained in CA_3, oxygen anions are arranged in a hexagonally close-packed lattice with aluminum ions occupying the octahedral interstices only [21-24]. Therefore, the spinel phase in CA_3 as with CA_2

only own six coordinated octahedral aluminum, while CA_3-U owns both four and six coordinated aluminum. The Al_{Td}/Al_{Oh} ratio is about 41/59 in CA_3-U which was calculated by peak area integration analysis.

Table 1 Results of EXAFS curve-fitting analysis [a] and ^{27}Al NMR

Sample	*r* (Å)	*N*	σ^2 (Å^2)	Cu_{Td}/Cu_{Oh} [b]	Al_{Td}/Al_{Oh} [c]	Formula
CA_2	1.947	4.4	0.0052	80/20	0/100	$(Cu_{0.80})[Cu_{0.20}Al_2]O_4$
CA_3	1.945	4.4	0.0064	80/20	0/100	$(Cu_{0.80})[Cu_{0.20}Al_2]O_4$
CA_3-U	1.939	4.8	0.0027	60/40	41/59	$(Cu_{0.36}Al_{0.91})[Cu_{0.25}Al_{1.35}]V_{0.13}O_4$

[a] *r* and *N* represent bond distance and coordination number of the first shell (Cu-O), σ^2 means Debye-Waller factor.
[b] Cu_{Td}/Cu_{Oh} was calculated by equation $y*4+(1-y)*6=N$, where y=fraction of tetrahedral Cu^{2+}.
[c] Al_{Td}/Al_{Oh} originated from ^{27}Al NMR data.

To characterize the distribution of Cu ions, diffuse reflectance spectra were obtained. Fig. 5 shows the results of CA_3 and CA_3-U (CA_2 has similar diffuse reflectance spectra to CA_3). A strong absorbance at about 1600 nm and a very weak absorbance at about 800 nm are detected for all samples. Literature studies proved that Cu^{2+} ions in an "octahedral" environment show a low wavelength band between 700 and 900 nm, whereas cupric ions in a "tetrahedral" environment have an absorption band between 1300 and 1700 nm [9,25-27]. However, the octahedral Cu^{2+} has a lower extinction co-efficient compared to that of tetrahedral Cu^{2+} [26,28]. Thus, it is difficult to obtain a quantitative data of Cu^{2+} distribution. Nonetheless, the reflectance spectra has proved the presence of Cu^{2+} in both the tetrahedral and octahedral sites.

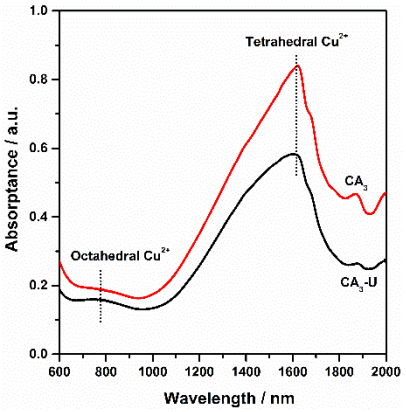

Fig. 5 Diffuse reflectance spectra of CA_3 and (CA_3-U).

Therefore, XAFS was performed in order to gain a quantitative estimation of the Cu^{2+} distribution in $CuAl_2O_4$, and the results are shown in Fig. 6 and Table 1. All three samples present similar Cu K-edge XANES spectra. A feature in the pre-edge region around 8977 eV is due to the dipole-forbidden transition 1s→3d [29,30], while the post-edge feature exhibits four well-resolved peaks at 8987, 8993, 8997 and 9002 eV owing to the 1s→4p transitions [31]. As was pointed out previously, the intensity of the pre-edge peak has a positive correlation with the fraction of tetrahedral Cu^{2+} [9,30]. Thus, it can be said that both CA_2 and CA_3 own more tetrahedral Cu^{2+} than CA_3-U, which is in agreement with reflectance results.

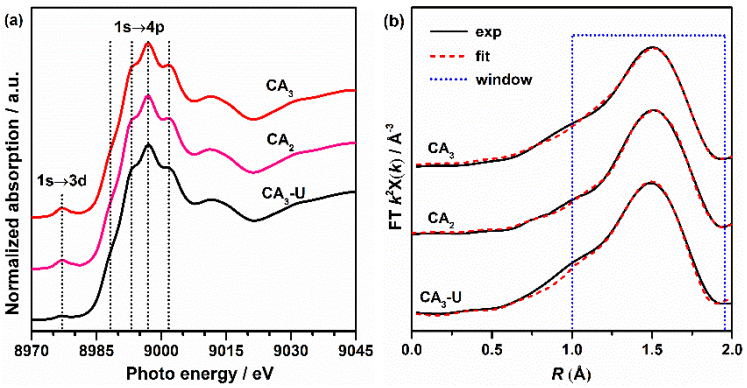

Fig. 6 (a) Cu K-edge XANES spectra and (b) EXAFS spectra with the best fitting of CA_2, CA_3 and CA_3-U.

The EXAFS data fitting analysis was performed in *R*-space for first coordination shell using the Demeter software package [32]. A hypothetical normal (Cu)[Al_2]O_4 spinel was used as the structural model. The analysis reveals that the coordination number is about 4.4 for both CA_2 and CA_3, while 4.8 for CA_3-U, which lead to a Cu_{Td}/Cu_{Oh} ratio of 80/20 and 60/40, respectively (Table 1). Therefore, by combining the ^{27}Al-NMR with EXAFS results, the structural formula of spinel phase in CA_2 or CA_3 can be written as $(Cu_{0.80})[Cu_{0.20}Al_2]O_4$, and $(Cu_{0.36}Al_{0.91})[Cu_{0.25}Al_{1.35}]V_{0.13}O_4$ (V means vacancy) for CA_3-U.

Further identification of these results was performed with Rietveld refinement of the XRD data using GSAS software [33,34]. By changing the cation distribution (occupancy in the refinement process), different structural models were used. The Rietveld refinement profiles and results are presented in Fig. 7 and Table 2, respectively. Interestingly, the Cu^{2+} and Al^{3+} distributions were found to be in good agreement with those of EXAFS curve fitting analysis, indicating the convincing structural results of spinel characterized by both NMR and EXAFS.

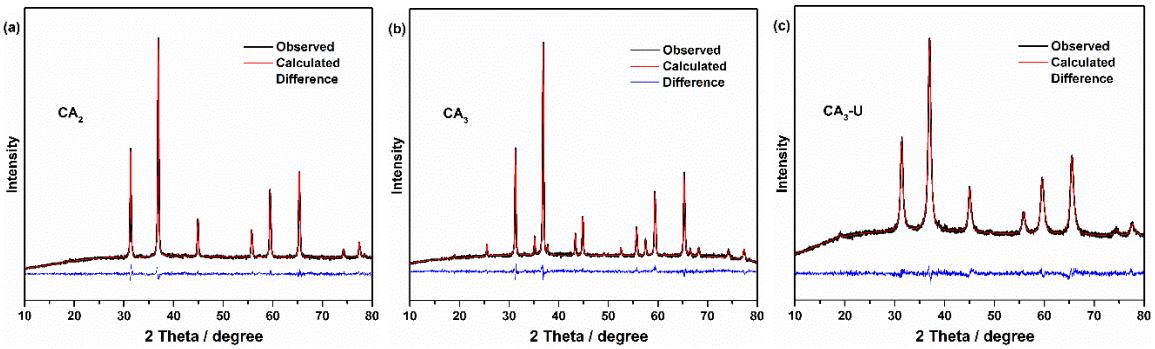

Fig. 7 XRD Rietveld refinement results of CA_2 (a), CA_3 (b) and CA_3-U (c).

Table 2 Results of XRD Rietveld refinement [a]

Sample	*a* (Å)	u	*R*p (%)	w*R*p (%)	Cu_{Td}/Cu_{Oh} [b]	Al_{Td}/Al_{Oh} [c]	Formula
CA_2	8.082	0.2594	3.36	4.29	82/18	0/100	$(Cu_{0.82})[Cu_{0.18}Al_2]O_4$
CA_3	8.077	0.2592	3.88	4.91	80/20	0/100	$(Cu_{0.80})[Cu_{0.20}Al_2]O_4$
CA_3-U	8.053	0.2606	2.41	3.07	58/42	42/58	$(Cu_{0.37}Al_{0.90})[Cu_{0.24}Al_{1.36}]V_{0.13}O_4$

[a] *a* represents the cell parameter of $CuAl_2O_4$, u represents the oxygen parameter, *R*p and w*R*p means residual and weighted residual.

On the basis of the above results, the structural formula of spinel phase in CA_2 or CA_3 can be written as $(Cu_{0.80})[Cu_{0.20}Al_2]O_4$, which only contain octahedral Al ions and show abnormal occupancies. According to previous literature studies, the properties of a spinel such as $MnFe_2O_4$, $Mn_{1-x}Zn_xFe_2O_4$ strongly depend on the cation distribution [35,36]. Therefore, the finding of an unusual cation distribution may provide a new insight for seeking special spinels which have distinctive properties and applications.

4. Conclusions

In summary, we report the first synthesis of $CuAl_2O_4$ with an unusual cation distribution, which is prepared by a solid phase reaction method. Thorough characterizations focused on the coordination environment of cations have led to a $(Cu_{1-x})[Cu_xAl_2]O_4$ (x=0.18-0.20) spinel with abnormal site occupancies. In addition, the cation distributions should be derived from the characterization of both cations for such special spinels.

5. Acknowledgements

This work has been financially supported by the National Natural Science Foundation of China (Grant No.: 21503254 and 21673270). XAFS characterization was performed at 1W1B endstation of Beijing Synchrotron Radiation Facility (BSRF), Institute of High Energy Physics, Chinese Academy of Sciences. Professor Mei Dong, Dr. Zhiwei Wu and Mrs Jie Gao are acknowledged for their support in XAFS measurements and data processing. Thanks are also extended to professor Weibin Fan, Yue He and Dr. Pengfei Wang for their help in collecting diffuse reflectance and 27 Al NMR data.

6. References

[1] M. Matsukata, S. Uemiya, E. Kikucht, Copper-Alumina spinel catalysts for steam reforming of methanol, Chem. Lett., 1988,17: 761-764.
[2] Y.-H. Huang, S.-F. Wang, A.-P. Tsai, S. Kameoka, Reduction behaviors and catalytic properties for methanol steam reforming of Cu-based spinel compounds CuX_2O_4 (X = Fe, Mn, Al, La), Ceram. Int., 2014, 40: 4541-4551.
[3] L. Li, X. Dong, Y. Dong, et al., Thermal conversion of hazardous metal copper via the preparation of $CuAl_2O_4$ spinel-based ceramic membrane for potential stabilization of simulated copper-rich waste, ACS Sustain. Chem. Eng., 2015, 3: 2611-2618.
[4] H.-J. Woelk, B. Hoffmann, G. Mestl, R. Schloegl, Experimental archaeology: investigation on the copper-aluminum-silicon-oxygen system, J. Am. Ceram. Soc., 2002, 85: 1876-1878.
[5] A. H. Piracha, S. M. Ramay, S. Atiq, et al., Dielectric and magnetic investigations of mixed cubic spinel Co-ferrites with controlled Mg content, J. Electroceram., 2015, 34: 122-129.
[6] D. H. K. Reddy, Y. S. Yun, Coordin. Chem. Rev., Spinel ferrite magnetic adsorbents: alternative future materials for water purification, 2016, 315: 90-111.
[7] E. Stefan, P. A. Connor, A. K. Azad, J. T. S. Irvine, Structure and properties of $MgM_xCr_{2-x}O_4$ (M= Li, Mg, Ti, Fe, Cu, Ga) spinels for electrode supports in solid oxide fuel cells, J. Mater. Chem. A, 2014, 2: 18106-18114.
[8] K. E. Sickafus, J. M. Wills, Structure of spinel, J. Am. Ceram. Soc., 1999, 82: 3279-3292.
[9] K.-I. Shimizu, H. Maeshima, H. Yoshida, et al., Spectroscopic characterization of Cu-Al_2O_3 catalysts for selective catalytic reduction of NO with propene Phys. Chem. Chem. Phys., 2000, 2: 2435-2439.
[10] E. C. Marques, R. M. Friedman, D. J. Dahm, The structure of copper aluminate: cation distribution at different temperatures and its implications for $Cu/A1_2O_3$ catalysts, Appl. Catal., 1985, 19: 387-403.
[11] R. M. Friedman, J. J. Freeman, F. W. Lytle. Characterization of $CuAl_2O_3$ catalysts, J. Catal., 1978, 55: 10-28.
[12] R. A. Fregola, F. Bosi, H. Skogby, U. Halenius, Cation ordering over short-range and long-range scales in the $MgAl_2O_4$-$CuAl_2O_4$ series, Am.Mineral., 2012, 97: 1821-1827.
[13] H. S. C. O'Neill, M. James, W. A. Dollase, S. A. T. Redfern, Temperature dependence of the cation distribution in $CuAl_2O_4$ spinel, Eur. J. Mineral., 2005, 17: 581-586.
[14] R. F. Cooley, J. S. Reed, Equilibrium cation distribution in $NiAl_2O_4$, $CuAl_2O_4$, and $ZnAl_2O_4$ spinels, J. Am. Ceram. Soc., 1972, 55: 395-398.
[15] T. Mimani, J. Alloys. Instant synthesis of nanoscale spinel aluminates, Compd, 2001, 315: 123-128.
[16] E. Ghanti, R. Nagarajan, Synthesis of $CuAl_2(acac)_4(OiPr)_4$, its hydrolysis and formation of bulk $CuAl_2O_4$ from the hydrolyzed gels; a case study of molecules to materials, Dalton. Trans., 2010, 39: 6056-6061.
[17] H. Xi, X. Hou, Y. Liu, et al., Cu-Al spinel oxide as an efficient catalyst for methanol steam reforming, Angew. Chem. Int. Ed., 2014, 53: 11886-11889.
[18] G. C. Gobbi, R. Christoffersen, M. T. Otten, et al., Direct determination of cation disorder in $MgAl_2O_4$ spinel by high-resolution 27Al magic-angle-spinning NMR spectroscopy, Chem. Lett., 1985, 14: 771-774.
[19] H. Furuhashi, M. Inagaki, S. Naka, Determination of cation distribution in spinels by X-ray diffraction method, J. Inorg. Nucl. Chem., 1973, 35: 3009-3014.
[20] V. Sepelak, S. Indris, I. Bergmann, et al., Nonequilibrium cation distribution in nanocrystalline $MgAl_2O_4$ spinel studied by 27Al magic-angle spinning NMR, Solid State Ionics., 2006, 177: 2487-2490.
[21] M. R. Hill, T. J. Bastow, S. Celotto, A. J. Hill, Integrated study of the calcination cycle from gibbsite to corundum, Chem. Mater., 2007, 19: 2877-2883.
[22] L.H. Chagas, G.S.G. D. Carvalho, R.A.S. S. Gil, et al., Obtaining aluminas from the thermal decomposition of their different precursors: An 27 Al MAS NMR and X-ray powder diffraction studies, Mater. Res. Bull., 2014, 49: 216-222.
[23] L.A. O'Dell, S.L. Savin, A.V. Chadwick, M.E. Smith, A 27Al MAS NMR study of a sol-gel produced alumina: Identification of the NMR parameters of the θ-Al_2O_3 transition alumina phase, Solid State Nucl. Mag., 2007, 31: 169-173.
[24] M.-H. Lee, C.-F. Cheng, V. Heine, J. Klinowski, Distribution of tetrahedral and octahedral A1 sites in gamma alumina, Chem. Phys. Lett., 1997, 265: 673-676.
[25] M. C. Marion, E. Garbowski, M. Primet, Physicochemical properties of copper oxide loaded alumina in methane combustion, J. Chem. Soc. Faraday Trans., 1990, 86: 3027-3032.
[26] J. J. Freeman, R. M. Friedman, Re-examination of the diffuse reflectance spectra of Cu/Al_2O_3 catalysts, J. Chem. Soc. Faraday Trans., 1978, 74: 758-761.

[27] I. Mindru, D. Gingasu, L. Patron, et al., Copper aluminate spinel by soft chemical routes, Ceram. Int., 2016, 42: 154-164.
[28] R. Pappalardo, Absorption spectra of Cu^{2+} in different crystal coordinations, J. Mol. Spectrosc, 1961, 6: 554-571.
[29] J. E. Hahn, R. A. Scott, K. O. Hodgson, Observation of an electric quadrupole transition in the X-ray absorption spectrum of a Cu (II) complex, Chem. Phys. Lett., 1982, 88: 595-598.
[30] A. L. Roe, D. J. Schneider, R. J. Mayer, et al., X-ray absorption spectroscopy of iron-tyrosinate proteins, J. Am. Chem. Soc, 1984, 106: 1676-1681.
[31] N. Kosugi, H. Kondoh, H. Tajima, H. Kuroda, Cu K-edge XANES of $(La_{1-x}Sr_x)_2CuO_4$, $YBa_2Cu_3O_y$ and related Cu oxides. valence, structure and final-state effects on 1s-4pπ and 1s-4pσ absorption, Chem. Phys., 1989, 135: 149-160.
[32] B. Ravel, M. Newville, ATHENA, ARTEMIS, HEPHAESTUS: data analysis for X-ray absorption spectroscopy using IFEFFIT, J. Synchrotron Radiat., 2005, 12: 537-541.
[33] A.C. Larson, R.B. Von Dreele, Gsas, Los Alamos National Laboratory Report LAUR, 1994.
[34] B. H. Toby, EXPGUI, a graphical user interface for GSAS, J. Appl. Cryst., 2001, 34: 210-213.
[35] J. Li, H. Yuan, G. Li, et al., Cation distribution dependence of magnetic properties of sol-gel prepared $MnFe_2O_4$ spinel ferrite nanoparticles, J. Magn. Magn. Mater., 2010, 322: 3396-3400.
[36] C. Rath, S. Anand, R. P. Das, et al., Dependence on cation distribution of particle size, lattice parameter, and magnetic properties in nanosize Mn-Zn ferrite, J. Appl. Phys., 2002, 91: 2211-2215.